NANO LETTERS

pubs.acs.org/NanoLett

Letter

Giant Enhancement of Continuous Wave Second Harmonic Generation from Few-Layer GaSe Coupled to High-*Q* Quasi Bound States in the Continuum

Zhuojun Liu,[§] Jiayi Wang,[§] Bo Chen, Yuming Wei,* Wenjing Liu, and Jin Liu*

Cite This: *Nano Lett.* 2021, 21, 7405−7410

Read Online

ACCESS | Metrics & More | Article Recommendations | Supporting Information

ABSTRACT: Two-dimensional (2D) layered materials such as GaSe recently have emerged as novel nonlinear optical materials with exceptional properties. Although exhibiting large nonlinear susceptibilities, the nonlinear responses of 2D materials are generally limited by the short interaction lengths with light, thus further enhancement via resonant photonic nanostructures is highly desired for building high-efficiency nonlinear devices. Here, we demonstrate a giant second-harmonic generation (SHG) enhancement by coupling 2D GaSe flakes to silicon metasurfaces supporting quasi-bound states in the continuum (quasi-BICs) under continuous-wave (CW) operation. Taking advantage of both high-quality factors and large mode areas of quasi-BICs, SHG from a GaSe flake is uniformly enhanced by nearly 4 orders of magnitude, which is promising for high-power coherent light sources. Our work provides an effective approach for enhancing nonlinear optical processes in 2D materials within the framework of silicon photonics, which also brings second-order nonlinearity associated with 2D materials to silicon photonic devices.

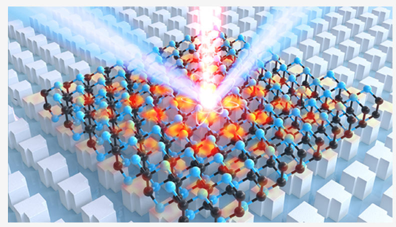

KEYWORDS: *Silicon metasurfaces, two-dimensional materials, bound states in the continuum, second harmonic generation*

INTRODUCTION

Nonlinear optics is one of the cornerstones of modern photonics which founded a broad range of applications in laser technology, optical microscopy, and quantum optics. Particularly, second harmonic generation (SHG) corresponds to the nonlinear process that converts two identical photons into one photon with doubled frequency.[1,2] As a widely observed second order nonlinear effect, SHG has been extensively applied in optical spectroscopy, signal processing, and image processing.[3−5] Conventional SHG devices generally rely on bulk nonlinear crystals including lithium niobate ($LiNbO_3$), beta barium borate (BBO), and potassium dihydrogen phosphate (KDP),[6−10] requiring phase-matching condition and long interaction length with light.

Recently, 2D layered materials including transition metal dichalcogenides (TMDCs) and gallium monochalcogenides are emerging as a promising tool in building on-chip nonlinear devices with ultrasmall footprints due to their ultrathin thicknesses and large nonlinear susceptibilities.[11] Among them, 2D gallium selenide (GaSe) exhibits a giant monolayer $\chi^{(2)}$ of ~1700 pm V^{-1} under telecom-band excitation,[12] demonstrating exceptional performances for high-efficiency SHG.[13−16] In particular, GaSe with ε-type stacking is always noncentrosymmetric for arbitrary layer thickness. Therefore, the strength of $\chi^{(2)}$ of ε-GaSe can be effectively enhanced by increasing the layer number.[12,17−19]

Nevertheless, nonlinear optical responses in 2D materials are seriously limited by their short interaction lengths with light. Photonic resonators and cavities can tightly confine light both spatially and temporally, hence serve as an effective approach to significantly enhance nonlinear optical interactions at the nanoscale. In general, in a 2D photonic structure without the requirement of phase matching, the SH field can be expressed as

$$\mathbf{P}(2\omega) \propto \int_V \chi^{(2)}(\mathbf{r}, \omega)[\mathbf{E}_{\mathrm{loc}}(\mathbf{r}, \omega)]^2 \mathrm{d}V \tag{1}$$

where $\mathbf{P}(2\omega)$ represents the SH field, $\chi^{(2)}$ is the second-order nonlinear susceptibility of material, $\mathbf{E}_{\mathrm{loc}}(\mathbf{r},\omega)$ denotes the local electric field of pump light, and V is the interaction volume.[20] Compared to other optical cavities and resonators such as photonic crystal nanocavities, metasurfaces enable uniform field enhancement over a large area, therefore allowing high-efficiency nonlinear processes with high operation power. While most of the early research focused on plasmonic metasurfaces due to their strong enhancement of $\mathbf{E}_{\mathrm{loc}}(\mathbf{r},\omega)$,[21−25] all-dielectric metasurfaces with much higher Q-factors provide an alternative platform for effective nonlinear interactions with low heat generations and high damage thresholds.[26−28] In particular, recent studies on photonic BICs

Received: May 20, 2021
Revised: July 2, 2021
Published: July 7, 2021

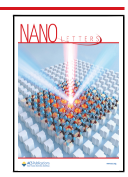

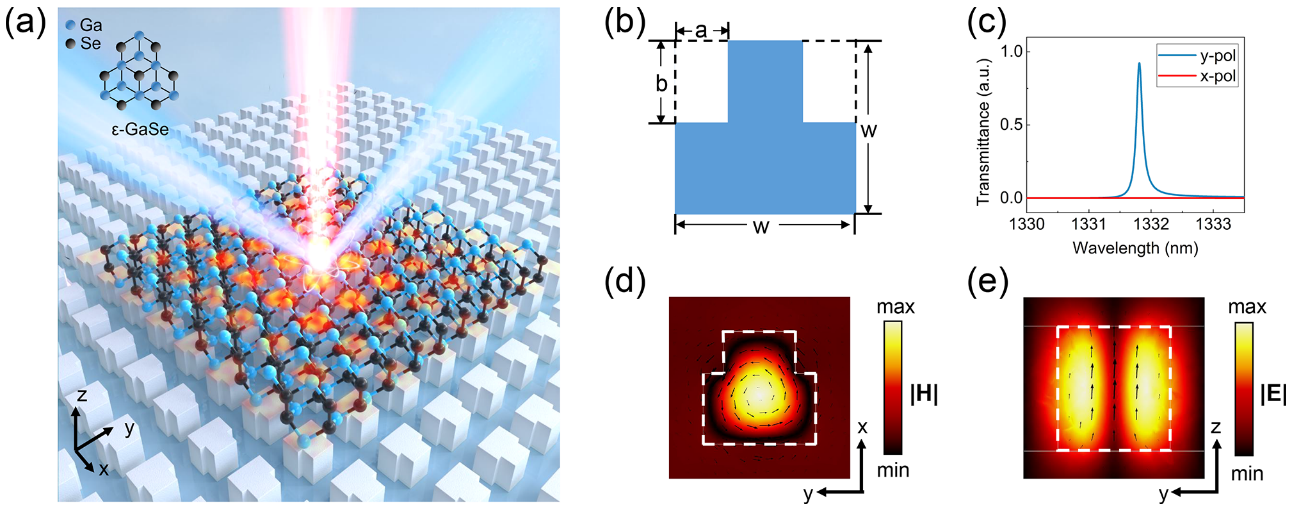

Figure 1. Hybrid device for enhancing the SHG. (a) Illustration of SHG from a GaSe flake laid on the surface of a Si metasurface consist of a periodic square lattice of T-shaped pillars. Inset: Lattice structure of ε-GaSe flake. (b) Diagram of the designed unit cell (the width w and the asymmetry parameters a and b). (c) Simulated transmission spectrum of x-polarized (red line) and y-polarized (blue line) excitations. (d) Simulated magnetic filed distribution at quasi-BIC mode in $x-y$ plane, the black arrows indicate in-plane electric field vectors. (e) Simulated electric field distribution at quasi-BIC mode in $y-z$ plane; the black arrows indicate in-plane magnetic field vectors.

in dielectric metasurfaces have proven their ultrahigh Q-factors and potential applications in low-threshold lasing,[29−32] sensing,[33−35] and enhancing both linear and nonlinear light−matter interactions.[36−41] BICs are exceptional localized states with energy embedded in but interestingly entirely decoupled from the radiative continuum often due to a symmetry mismatch between the resonant and radiative modes. While possessing theoretically infinite radiative Q-factors that are appealing in various applications, BICs suffer from the inaccessibility of external excitations. A slight symmetry breaking may be desired to transfer the symmetry-protected BICs into quasi-BICs with finite radiative losses, thereby reaching an optimum balance between the Q-factor and the in- and out-coupling efficiencies.[42−45]

As an ideal material for near-infrared dielectric metasurface, silicon has low optical loss, large refractive index, and mature fabrication techniques. In particular, in silicon metasurfaces BICs based on Mie-resonances have been employed to enhance the nonlinear processes, for instance, four-wave mixing and third harmonic generation.[46] However, even-order nonlinear susceptibilities vanish in bulk silicon due to the presence of centrosymmetry, which seriously limits its applications in nonlinear optics. Integrating 2D materials to silicon metasurfaces with delicately designed optical resonances offers an efficacious route to introduce the even-order nonlinearity to silicon photonics. Recently, by combining TMDCs with Si metasurfaces supporting low-Q quasi-BICs, SHG enhancement by 3 orders of magnitude was observed under femtosecond-pulse excitation.[47] Nonetheless, continuous-wave (CW) SHG is preferred in practical applications due to its low-power consumption, which to date is limited to an enhancement factor of 26 in low-Q metasurfaces.[19]

Here, we report a giant enhancement of CW SHG from 2D GaSe flakes utilizing a high-Q quasi-BIC with large mode area demonstrated in our recent work.[44] Si metasurfaces supporting quasi-BICs with Q-factors up to 8911 were fabricated in which symmetric defects are introduced in each unit cell to allow the transition from BIC to quasi-BIC. Layered GaSe flakes are then carefully transferred onto the metasurfaces without compromising their Q-factors. By tuning the excitation laser in resonance with the quasi-BIC, a giant enhancement of CW SHG up to ∼9400-fold is achieved compared to the same GaSe flake on the bare substrate. The polarization characteristics of the SHG further confirms that the enhancement is attributed to the quasi-BIC mode. Our work demonstrates the feasibility of developing nanoscale nonlinear photonic devices by integrating 2D materials with dielectric metasurfaces.

■ DEVICE DESIGN

The schematic of the hybrid structure is presented in Figure 1a in which the SHG from a GaSe flake is amplified by a Si metasurface composed of periodically arranged Si meta-atoms with symmetric defects. The introduction of defects breaks the rotational symmetry protection of BICs, transferring them into quasi-BICs that are accessible with free-space excitations at normal incidence.[44] To maintain the high-Q factor of the BICs, symmetric defects preserving the mirror symmetry in the $x-z$ plane was exploited. Specifically, each meta-atom is designed as a T-shaped pillar, as confirmed in Figure 1b, defined by the width w, and the asymmetry parameters a, b. As a result of the mirror symmetry, the quasi-BICs can only be excited by y-polarized beams, as shown in Figure 1c. Considering the nanofabrication resolution of ∼50 nm in our tools,[44] the parameters are designed as a = 70 nm, b = 140 nm, and w = 360 nm with the Si thickness of 400 nm and the lattice period $p_x = p_y$ = 580 nm.

The designed structure supports a quasi-BIC mode at the wavelength of 1331.8 nm with a theoretical Q-factor of 17 612, calculated by COMSOL Multiphysics. Moreover, as the simulated magnetic field distribution in the $x-y$ plane unfolds, the quasi-BIC mode has the nature of a magnetic dipole, which has been demonstrated to strongly enhance the nonlinear light−matter interactions,[48] as shown in Figure 1d. Figure 1e presents the simulated distribution in the $y-z$ plane of the electric field, where a considerable electric field enhancement can be noticed on the upper surface of a T-shaped pillar, ensuring efficient coupling with the GaSe flake.

https://doi.org/10.1021/acs.nanolett.1c01975
Nano Lett. 2021, 21, 7405−7410

RESULTS

Quasi-BIC metasurfaces of 19 × 19 Si meta-atom arrays are fabricated via e-beam lithography followed by plasma dry etching on a silicon-on-insulator (SOI) wafer consisting of a 400 nm top Si layer and 3 μm buried SiO_2 (Figure 2a). We use mechanical exfoliation method for the preparation of GaSe flakes, and then carefully transfer the flake onto metasurface using polydimethylsiloxane (PDMS) with a yield around 90%. Optical microscope image of the hybrid structure is presented in Figure 2b, showing that the metasurface is fully encapsulated by the GaSe flake. As shown in Figure 2c, the thickness of the GaSe flake is measured by an atomic force microscope as 21.6 nm, corresponding to 24 layers with the monolayer thickness of 0.89 nm.[49] It is worth noting that the GaSe flakes applied in the study exhibit ε-type stacking, which are always in the absence of centrosymmetry.[12] The observation of SHG from the GaSe shows no layer dependence and its intensity is linearly scaled with the layer number. To examine the influence of the GaSe flake on the quasi-BIC mode, we use the orthogonal polarization method, that is, placing two orthogonal polarizers at the excitation and collection paths, to obtain the reflection spectra of the metasurface with and without the GaSe flake. As is shown in Figure 2d, a redshift (~10 nm) of the quasi-BIC mode is observed after the encapsulation of GaSe flake due to the change of the environmental effective refractive index, while the degradation of the Q-factor is negligible. The successful integration of the relatively thick GaSe flake onto the Si metasurface without compromising the Q-factor is crucial to taking full advantages of the sharp resonances of the quasi-BICs in our work.

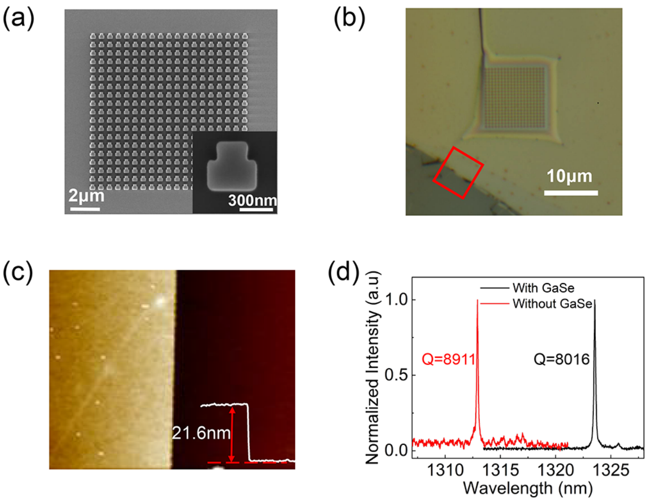

Figure 2. Characterizations of the Si metasurface and GaSe flake. (a) Top view scanning-electron micrograph of a 19 × 19 arrays Si metasurface. Inset: Enlarged image of a unit cell. (b) Optical microscope image of few-layer GaSe flake transferred onto the metasurface. (c) AFM image of the boundary of GaSe flake (red frame in (b)). The inset shows the measured thickness with a value of 21.6 nm, corresponding to the layer number of 24. (d) Reflection spectra for the quasi-BIC mode of metasurface with (black) and without (red) GaSe flake.

To characterize the SHG from the hybrid structure at room temperature, a CW laser (1260−1380 nm) was employed to pump the sample at 1.5 mW. The excitation laser was focused to a 3 μm-diameter spot via a 20× objective lens (NA = 0.45) to ensure the mode overlap between the incident spot and the quasi-BIC mode. The SHG signal in the reflected direction was collected and sent to a grating spectrometer (PISP 2758). Typical measured spectra of pump laser (red line) and the corresponding SH signal (yellow line) are shown in Figure 3a. It can be observed that an emission appears at 667.28 nm with fixed 1334.6 nm of the pump laser, which is an obvious evidence of frequency-doubled photons generation. Figure 3b shows the reflected SHG spectra of the GaSe flake on (blue line) and off (red line) the metasurface, respectively, confirming an ~9400-fold enhancement with the pump laser in resonance with the quasi-BIC. Third harmonic generation (THG) is certainly expected and should be also enhanced by the quasi-BICs in our experiment. However, the THG signal is not directly observed in our experiment due to the limited spectral coverage of our optical setup. It is noted that the SHG enhancement factor in our work is nearly 3 orders of magnitude higher than previous demonstration in the same material platform,[45] which is attributed to the much higher Q-factor of the quasi-BIC mode achieved in our hybrid system. The critical role played by the quasi-BIC in SHG enhancement is further confirmed by the wavelength dependent SHG measurement, as shown in Figure 3c. When scanning the pumping laser across the quasi-BIC wavelength, the SHG intensity changes drastically, reaching the maximum when the pump laser is in resonance with the quasi-BIC. The wavelength dependence of SHG strictly follows the profile of f_{Fano}^2, in which f_{Fano} represents the Fano fitting of the quasi-BIC mode. The nonlinear nature of the SHG process is verified by the pump power-dependent SHG measurement in a double logarithmic plot (Figure 3d). The exponent value of the power dependence is fitted to be $n = 1.97$ with $P_{\mathrm{SHG}} = mP_{\mathrm{pump}}^n$, demonstrating a quadratic dependence of the SHG intensity on the pump power.

Figure 4 displays the polarization characteristics of the SHG signal. Specifically, y-polarized SHG intensity is monitored when the polarization of the excitation laser rotates from 0° to 360°. The y-polarized SHG intensity of the GaSe flake on the metasurface is dominated by the polarization of the quasi-BIC, which comes to the maximum under a pump laser with y-polarized as well. On the contrary, the y-polarized SHG intensity follows a 4-fold rotational symmetry when pumping off the metasurface (Figure 4b), resulting from the crystalline symmetry of GaSe.[50] It should be noted that we deliberately aligned the polarization of the quasi-BIC mode to the arm-chair crystallographic axis of the GaSe flake in order to obtain the maximal SHG signal along the y-axis.

CONCLUSION

In conclusion, we demonstrated the successful integration of 2D GaSe flakes on Si metasurfaces supporting quasi-BIC modes without compromising their high-Q factors. The unique combination of the high Q-factor supported by the quasi-BIC mode and the large $\chi^{(2)}$ of the few-layered GaSe flake results in a giant enhancement of CW SHG as high as 9400-fold. Notably, such a record enhancement factor achieved in this work is nearly 3 orders of magnitude higher than previous reports in the same material platform. Our design not only significantly enhances the nonlinear responses of 2D materials by using high-Q optical resonances but also brings the second-order nonlinearity associated with 2D materials into silicon photonics. We believe that the fusion between 2D materials and dielectric metasurfaces supporting high-Q quasi-BICs is a

https://doi.org/10.1021/acs.nanolett.1c01975
Nano Lett. 2021, 21, 7405−7410

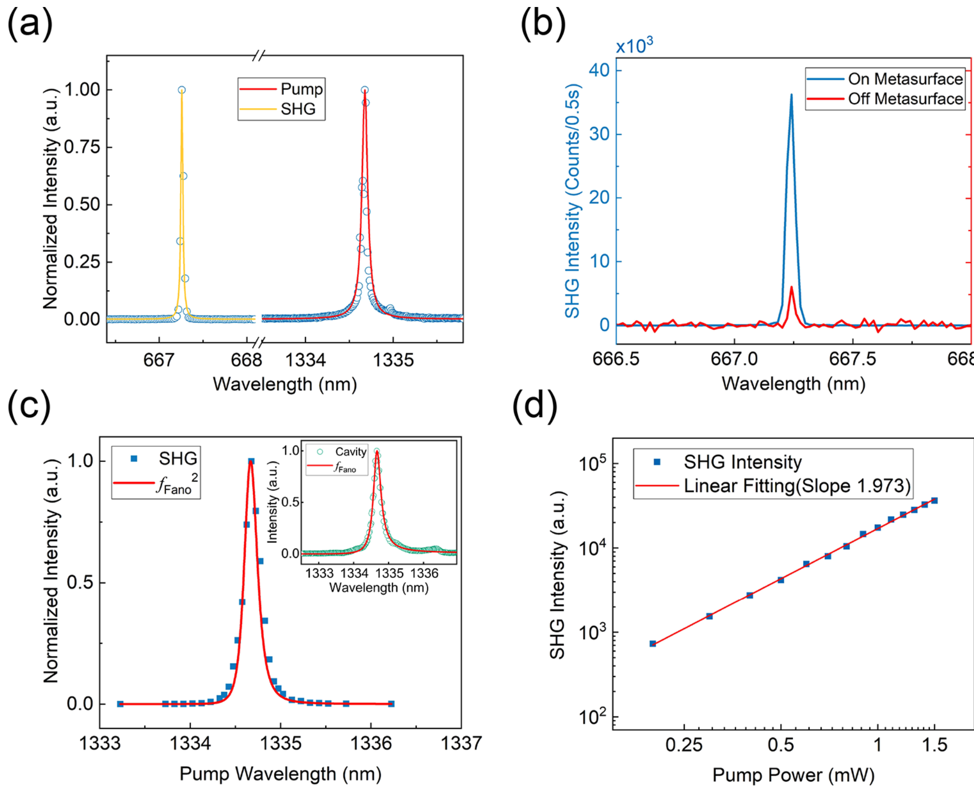

Figure 3. Quasi-BIC enhanced SHG. (a) Normalized spectra of fundamental laser (right) and SHG signal (left) generated from the hybrid structure of GaSe flake and metasurface at the quasi-BIC resonance. (b) Measured spectra of the SHG from GaSe flake on (blue, integral time 0.5 s) and off (red, integral time 20 s) the metasurface. (c) Dependence of SHG intensity on the pump wavelength. Inset shows the Fano fitting of the quasi-BIC mode. (d) Measured SHG intensities as a function of pump power. The exponent value obtained from the fitting is 1.973.

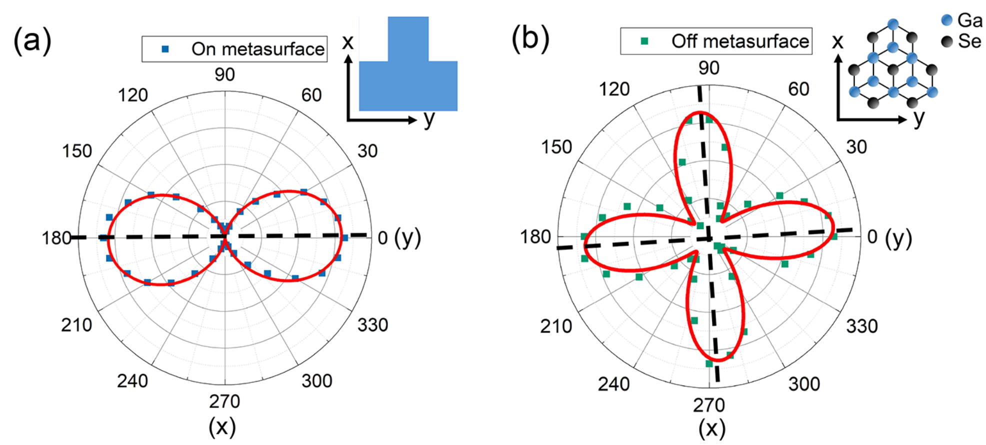

Figure 4. Intensities of SHG as a function of the pump beam polarization for the GaSe flake. (a) On metasurface and (b) off metasurface. 0° corresponds to the polarization parallel to the *y*-axis, which is the polarization of the quasi-BIC mode.

promising approach to develop integrated devices for nonlinear photonics and optoelectronics.[51]

■ ASSOCIATED CONTENT

Supporting Information

The Supporting Information is available free of charge at https://pubs.acs.org/doi/10.1021/acs.nanolett.1c01975.

> Additional details on sample fabrication of Si metasurfaces, optical setup for linear and nonlinear optical measurements; additional figures of the fabrication processes and the measurement setup (PDF)

■ AUTHOR INFORMATION

Corresponding Authors

Yuming Wei − *State Key Laboratory of Optoelectronic Materials and Technologies, School of Physics, Sun Yat-sen University, Guangzhou 510275, China*; Email: weiym8@mail.sysu.edu.cn

Jin Liu − *State Key Laboratory of Optoelectronic Materials and Technologies, School of Physics, Sun Yat-sen University, Guangzhou 510275, China*; orcid.org/0000-0001-5727-6874; Email: liujin23@mail.sysu.edu.cn

Authors

Zhuojun Liu − *State Key Laboratory of Optoelectronic Materials and Technologies, School of Physics, Sun Yat-sen University, Guangzhou 510275, China*

Jiayi Wang − *State Key Laboratory of Optoelectronic Materials and Technologies, School of Physics, Sun Yat-sen University, Guangzhou 510275, China*

Bo Chen − *State Key Laboratory of Optoelectronic Materials and Technologies, School of Physics, Sun Yat-sen University, Guangzhou 510275, China*

Wenjing Liu − *State Key Laboratory for Mesoscopic Physics and Frontiers Science Center for Nano-optoelectronics, School of Physics, Peking University, 100871 Beijing, China;* orcid.org/0000-0002-9441-8859

Complete contact information is available at: https://pubs.acs.org/10.1021/acs.nanolett.1c01975

Author Contributions

[§]Z.L. and J.W. contributed equally.

Notes

The authors declare no competing financial interest.

■ ACKNOWLEDGMENTS

This research was supported by National Key R&D Program of China (2018YFA0306100), the National Natural Science Foundation of China (11874437, 61935009), Guangzhou Science and Technology Project (201805010004), the Natural Science Foundation of Guangdong (2018B030311027), and the national supercomputer center in Guangzhou.

■ REFERENCES

(1) Boyd, R. W. *Nonlinear Optics*; Academic Press, 2020.

(2) Shen, Y.-R. *The Principles of Nonlinear Optics*; Wiley-Interscience: New York, 1984.

(3) Cao, Q.-T.; Liu, R.; Wang, H.; Lu, Y.-K.; Qiu, C.-W.; Rotter, S.; Gong, Q.; Xiao, Y.-F. Reconfigurable symmetry-broken laser in a symmetric microcavity. *Nat. Commun.* **2020**, *11* (1), 1−7.

(4) Chen, J.-h.; Shen, X.; Tang, S.-J.; Cao, Q.-T.; Gong, Q.; Xiao, Y.-F. Microcavity nonlinear optics with an organically functionalized surface. *Phys. Rev. Lett.* **2019**, *123* (17), 173902.

(5) Zhang, X.; Cao, Q.-T.; Wang, Z.; Liu, Y.-x.; Qiu, C.-W.; Yang, L.; Gong, Q.; Xiao, Y.-F. Symmetry-breaking-induced nonlinear optics at a microcavity surface. *Nat. Photonics* **2019**, *13* (1), 21−24.

(6) Kushwaha, S.; Shakir, M.; Maurya, K.; Shah, A.; Wahab, M.; Bhagavannarayana, G. Remarkable enhancement in crystalline perfection, second harmonic generation efficiency, optical transparency, and laser damage threshold in potassium dihydrogen phosphate crystals by L-threonine doping. *J. Appl. Phys.* **2010**, *108* (3), 033506.

(7) Su, R.; Zhu, M.; Huang, Z.; Wang, B.; Wu, W. Second harmonic generation efficiency affected by radiation force of a high-energy laser beam through stress within a mounted potassium dihydrogen phosphate crystal. *Opt. Eng.* **2018**, *57* (01), 1.

(8) Chen, J.; Han, P.; Zhang, X.-C. Terahertz-field-induced second-harmonic generation in a beta barium borate crystal and its application in terahertz detection. *Appl. Phys. Lett.* **2009**, *95* (1), 011118.

(9) Banks, P.; Feit, M.; Perry, M. High-intensity third-harmonic generation in beta barium borate through second-order and third-order susceptibilities. *Opt. Lett.* **1999**, *24* (1), 4−6.

(10) Miller, G.; Batchko, R.; Tulloch, W.; Weise, D.; Fejer, M.; Byer, R. 42%-efficient single-pass cw second-harmonic generation in periodically poled lithium niobate. *Opt. Lett.* **1997**, *22* (24), 1834−1836.

(11) Autere, A.; Jussila, H.; Dai, Y.; Wang, Y.; Lipsanen, H.; Sun, Z. Nonlinear optics with 2D layered materials. *Adv. Mater.* **2018**, *30* (24), 1705963.

(12) Zhou, X.; Cheng, J.; Zhou, Y.; Cao, T.; Hong, H.; Liao, Z.; Wu, S.; Peng, H.; Liu, K.; Yu, D. Strong second-harmonic generation in atomic layered GaSe. *J. Am. Chem. Soc.* **2015**, *137* (25), 7994−7997.

(13) Tang, Y.; Mandal, K. C.; McGuire, J. A.; Lai, C. W. Layer-and frequency-dependent second harmonic generation in reflection from GaSe atomic crystals. *Phys. Rev. B: Condens. Matter Mater. Phys.* **2016**, *94* (12), 125302.

(14) Hu, L.; Huang, X.; Wei, D. Layer-independent and layer-dependent nonlinear optical properties of two-dimensional GaX (X= S, Se, Te) nanosheets. *Phys. Chem. Chem. Phys.* **2017**, *19* (18), 11131−11141.

(15) Fang, L.; Yuan, Q.; Fang, H.; Gan, X.; Li, J.; Wang, T.; Zhao, Q.; Jie, W.; Zhao, J. Multiple Optical Frequency Conversions in Few-Layer GaSe Assisted by a Photonic Crystal Cavity. *Adv. Opt. Mater.* **2018**, *6* (22), 1800698.

(16) Jiang, B.; Hao, Z.; Ji, Y.; Hou, Y.; Yi, R.; Mao, D.; Gan, X.; Zhao, J. High-efficiency second-order nonlinear processes in an optical microfibre assisted by few-layer GaSe. *Light: Sci. Appl.* **2020**, *9* (1), 1−8.

(17) Jie, W.; Chen, X.; Li, D.; Xie, L.; Hui, Y. Y.; Lau, S. P.; Cui, X.; Hao, J. Layer-dependent nonlinear optical properties and stability of non-centrosymmetric modification in few-layer GaSe sheets. *Angew. Chem.* **2015**, *127* (4), 1201−1205.

(18) Jiang, B.; Hao, Z.; Ji, Y.; Hou, Y.; Yi, R.; Mao, D.; Gan, X.; Zhao, J. High-efficiency second-order nonlinear processes in an optical microfibre assisted by few-layer GaSe. *Light: Sci. Appl.* **2020**, *9* (1), 1−8.

(19) Yuan, Q.; Fang, L.; Fang, H.; Li, J.; Wang, T.; Jie, W.; Zhao, J.; Gan, X. Second harmonic and sum-frequency generations from a silicon metasurface integrated with a two-dimensional material. *ACS Photonics* **2019**, *6* (9), 2252−2259.

(20) Yang, Y.; Wang, W.; Boulesbaa, A.; Kravchenko, I. I.; Briggs, D. P.; Puretzky, A.; Geohegan, D.; Valentine, J. Nonlinear Fano-resonant dielectric metasurfaces. *Nano Lett.* **2015**, *15* (11), 7388−7393.

(21) Lee, J.; Tymchenko, M.; Argyropoulos, C.; Chen, P.-Y.; Lu, F.; Demmerle, F.; Boehm, G.; Amann, M.-C.; Alu, A.; Belkin, M. A. Giant nonlinear response from plasmonic metasurfaces coupled to intersubband transitions. *Nature* **2014**, *511* (7507), 65−69.

(22) Kruk, S.; Weismann, M.; Bykov, A. Y.; Mamonov, E. A.; Kolmychek, I. A.; Murzina, T.; Panoiu, N. C.; Neshev, D. N.; Kivshar, Y. S. Enhanced magnetic second-harmonic generation from resonant metasurfaces. *ACS Photonics* **2015**, *2* (8), 1007−1012.

(23) Black, L.-J.; Wiecha, P. R.; Wang, Y.; De Groot, C.; Paillard, V.; Girard, C.; Muskens, O. L.; Arbouet, A. Tailoring second-harmonic generation in single L-shaped plasmonic nanoantennas from the capacitive to conductive coupling regime. *ACS Photonics* **2015**, *2* (11), 1592−1601.

(24) Hu, G.; Hong, X.; Wang, K.; Wu, J.; Xu, H.-X.; Zhao, W.; Liu, W.; Zhang, S.; Garcia-Vidal, F.; Wang, B.; et al. Coherent steering of nonlinear chiral valley photons with a synthetic Au-WS 2 metasurface. *Nat. Photonics* **2019**, *13* (7), 467−472.

(25) Wang, Z.; Dong, Z.; Gu, Y.; Chang, Y.-H.; Zhang, L.; Li, L.-J.; Zhao, W.; Eda, G.; Zhang, W.; Grinblat, G.; Maier, S. A.; Yang, J. K. W.; Qiu, C.-W.; Wee, A. T. S. Giant photoluminescence enhancement in tungsten-diselenide-gold plasmonic hybrid structures. *Nat. Commun.* **2016**, *7* (1), 1−8.

(26) Liu, H.; Guo, C.; Vampa, G.; Zhang, J. L.; Sarmiento, T.; Xiao, M.; Bucksbaum, P. H.; Vučković, J.; Fan, S.; Reis, D. A. Enhanced high-harmonic generation from an all-dielectric metasurface. *Nat. Phys.* **2018**, *14* (10), 1006−1010.

(27) Liu, S.; Vabishchevich, P. P.; Vaskin, A.; Reno, J. L.; Keeler, G. A.; Sinclair, M. B.; Staude, I.; Brener, I. An all-dielectric metasurface as a broadband optical frequency mixer, (1). *Nat. Commun.* **2017**, *9* (1), 1−6.

(28) Shcherbakov, M. R.; Liu, S.; Zubyuk, V. V.; Vaskin, A.; Vabishchevich, P. P.; Keeler, G.; Pertsch, T.; Dolgova, T. V.; Staude,

I.; Brener, I.; Fedyanin, A. A.; et al. Ultrafast all-optical tuning of direct-gap semiconductor metasurfaces. *Nat. Commun.* **2017**, *8* (1), 1−6.

(29) Ha, S. T.; Fu, Y. H.; Emani, N. K.; Pan, Z.; Bakker, R. M.; Paniagua-Domínguez, R.; Kuznetsov, A. I. Directional lasing in resonant semiconductor nanoantenna arrays. *Nat. Nanotechnol.* **2018**, *13* (11), 1042−1047.

(30) Kodigala, A.; Lepetit, T.; Gu, Q.; Bahari, B.; Fainman, Y.; Kanté, B. Lasing action from photonic bound states in continuum. *Nature* **2017**, *541* (7636), 196−199.

(31) Wang, Y.; Fan, Y.; Zhang, X.; Tang, H.; Song, Q.; Han, J.; Xiao, S. Highly Controllable Etchless Perovskite Microlasers Based on Bound States in the Continuum. *ACS Nano* **2021**, *15* (4), 7386−7391.

(32) Huang, C.; Zhang, C.; Xiao, S.; Wang, Y.; Fan, Y.; Liu, Y.; Zhang, N.; Qu, G.; Ji, H.; Han, J.; et al. Ultrafast control of vortex microlasers. *Science* **2020**, *367* (6481), 1018−1021.

(33) Liu, Y.; Zhou, W.; Sun, Y. Optical refractive index sensing based on high-Q bound states in the continuum in free-space coupled photonic crystal slabs. *Sensors* **2017**, *17* (8), 1861.

(34) Yesilkoy, F.; Arvelo, E. R.; Jahani, Y.; Liu, M.; Tittl, A.; Cevher, V.; Kivshar, Y.; Altug, H. Ultrasensitive hyperspectral imaging and biodetection enabled by dielectric metasurfaces. *Nat. Photonics* **2019**, *13* (6), 390−396.

(35) Chen, Y.; Zhao, C.; Zhang, Y.; Qiu, C.-w. Integrated Molar Chiral Sensing Based on High-Q Metasurface. *Nano Lett.* **2020**, *20* (12), 8696−8703.

(36) Liu, S.; Vaskin, A.; Addamane, S.; Leung, B.; Tsai, M.-C.; Yang, Y.; Vabishchevich, P. P.; Keeler, G. A.; Wang, G.; He, X.; et al. Light-emitting metasurfaces: simultaneous control of spontaneous emission and far-field radiation. *Nano Lett.* **2018**, *18* (11), 6906−6914.

(37) Yuan, S.; Qiu, X.; Cui, C.; Zhu, L.; Wang, Y.; Li, Y.; Song, J.; Huang, Q.; Xia, J. Strong photoluminescence enhancement in all-dielectric Fano metasurface with high quality factor. *ACS Nano* **2017**, *11* (11), 10704−10711.

(38) Vabishchevich, P. P.; Liu, S.; Sinclair, M. B.; Keeler, G. A.; Peake, G. M.; Brener, I. Enhanced second-harmonic generation using broken symmetry III-V semiconductor fano metasurfaces. *ACS Photonics* **2018**, *5* (5), 1685−1690.

(39) Anthur, A. P.; Zhang, H.; Paniagua-Dominguez, R.; Kalashnikov, D. A.; Ha, S. T.; Maß, T. W.; Kuznetsov, A. I.; Krivitsky, L. Continuous Wave Second Harmonic Generation Enabled by Quasi-Bound-States in the Continuum on Gallium Phosphide Metasurfaces. *Nano Lett.* **2020**, *20* (12), 8745−8751.

(40) Pertsch, T.; Kivshar, Y. Nonlinear optics with resonant metasurfaces. *MRS Bull.* **2020**, *45* (3), 210−220.

(41) Muhammad, N.; Chen, Y.; Qiu, C.-W.; Wang, G. P. Optical Bound States in Continuum in MoS2-Based Metasurface for Directional Light Emission. *Nano Lett.* **2021**, *21* (2), 967−972.

(42) Marinica, D.; Borisov, A.; Shabanov, S. Bound states in the continuum in photonics. *Phys. Rev. Lett.* **2008**, *100* (18), 183902.

(43) Koshelev, K.; Lepeshov, S.; Liu, M.; Bogdanov, A.; Kivshar, Y. Asymmetric metasurfaces with high-Q resonances governed by bound states in the continuum. *Phys. Rev. Lett.* **2018**, *121* (19), 193903.

(44) Liu, Z.; Xu, Y.; Lin, Y.; Xiang, J.; Feng, T.; Cao, Q.; Li, J.; Lan, S.; Liu, J. High-Q quasibound states in the continuum for nonlinear metasurfaces. *Phys. Rev. Lett.* **2019**, *123* (25), 253901.

(45) Campione, S.; Liu, S.; Basilio, L. I.; Warne, L. K.; Langston, W. L.; Luk, T. S.; Wendt, J. R.; Reno, J. L.; Keeler, G. A.; Brener, I.; et al. Broken symmetry dielectric resonators for high quality factor Fano metasurfaces. *ACS Photonics* **2016**, *3* (12), 2362−2367.

(46) Leuthold, J.; Koos, C.; Freude, W. Nonlinear silicon photonics. *Nat. Photonics* **2010**, *4* (8), 535−544.

(47) Bernhardt, N.; Koshelev, K.; White, S. J.; Meng, K. W. C.; Froch, J. E.; Kim, S.; Tran, T. T.; Choi, D.-Y.; Kivshar, Y.; Solntsev, A. S. Quasi-BIC resonant enhancement of second-harmonic generation in WS2 monolayers. *Nano Lett.* **2020**, *20* (7), 5309−5314.

(48) Shcherbakov, M. R.; Neshev, D. N.; Hopkins, B.; Shorokhov, A. S.; Staude, I.; Melik-Gaykazyan, E. V.; Decker, M.; Ezhov, A. A.; Miroshnichenko, A. E.; Brener, I.; et al. Enhanced third-harmonic generation in silicon nanoparticles driven by magnetic response. *Nano Lett.* **2014**, *14* (11), 6488−6492.

(49) Gan, X.-T.; Zhao, C.-Y.; Hu, S.-Q.; Wang, T.; Song, Y.; Li, J.; Zhao, Q.-H.; Jie, W.-Q.; Zhao, J.-L. Microwatts continuous-wave pumped second harmonic generation in few-and mono-layer GaSe. *Light: Sci. Appl.* **2018**, *7* (1), 17126−17126.

(50) Deka, J.; Dandu, M.; AS, L. K.; Menon, S.; Jyothsna, K.; Biswas, R.; Majumdar, K.; Raghunathan, V. Polarization independent enhancement of zeroth order diffracted second harmonic from multilayer gallium selenide on a silicon resonant metasurface. *Opt. Express* **2020**, *28* (24), 35695−35707.

(51) Cazzanelli, M.; Schilling, J. Second order optical nonlinearity in silicon by symmetry breaking. *Appl. Phys. Rev.* **2016**, *3* (1), 011104.

https://doi.org/10.1021/acs.nanolett.1c01975
Nano Lett. 2021, 21, 7405−7410